Comparative Analysis of Radial and Tangential Diffuser Centrifugal Pumps, at Varying Specific Speeds

Ali Kibar

Kocaeli University, Department of Mechanical and Material Technologies, Uzunciftlik Nuh Cimento Campus, Kocaeli, 41180, Türkiye, alikibar@kocaeli.edu.tr

Kadri Suleyman Yigit

Kocaeli University, Department of Mechanical Engineering, Umuttepe Campus, Kocaeli, 41001, Türkiye, kyigit@kocaeli.edu.tr

Abstract: In this study, three centrifugal pumps, with specific speeds – dimensionless parameters used to assess pump performance – of 19, 27 and 42, were numerically investigated to evaluate the influence of diffuser type on radial-flow pump performance. For each specific speed, the radial and tangential diffuser configurations were paired with identical impeller geometry, ensuring a one-to-one comparison at the same head (20 m) and rotational speed (2800 rpm). The specific speeds correspond to flow rates of 250, 500, and 1200 L/min, respectively. The results show that low specific speeds exhibit greater unsteadiness, with head fluctuations decreasing from approximately 4 m at n_q : 19 to approximately 0.5 m at n_q : 42. At low specific speeds, the radial diffuser generates a higher head due to reduced flow separation; however, as specific speed increases, the tangential diffuser produces a higher head, consistent with its ability to accommodate stronger tangential momentum. Although the radial diffuser displays slightly larger instantaneous head fluctuations at n_q : 27 and 42, it experiences lower hydrodynamic force levels than the tangential diffuser at the same operating conditions. This distinction highlights that head fluctuation and surface-integrated force response are governed by different mechanisms. The systematic comparison across three specific speeds provides new insight into diffuser selection, demonstrating that appropriate diffuser geometry enhances hydraulic efficiency, suppresses unsteady flow structures, and reduces loading on volute surfaces. These findings provide practical guidance for the design of diffusers in centrifugal pumps.

Keywords: centrifugal pump; radial flow; specific speed; numerical analysis; flow stability

1 Introduction

Pumps are mechanical devices used to transfer fluids from one place to another. They are typically categorized into two main groups: positive-displacement pumps and dynamic pumps [1]. Among dynamic pumps, centrifugal pumps are the most widely used due to their high efficiency and reliable performance [2]. Their operation is based on the pressure rise generated by the rotating impeller, which drives the fluid from the inlet to the outlet. A centrifugal pump primarily consists of a volute casing and a rotating impeller [3], and its performance is strongly influenced by the designs of both components. The volute plays a critical role in converting the kinetic energy of the fluid exiting the impeller into pressure energy through the gradual expansion of the spiral passage [1] [4]. This controlled diffusion process enhances pressure recovery and reduces hydraulic losses.

Two common volute configurations are tangential diffusers (Figure 1a) and radial diffusers (Figure 1b), both of which are used under different operating conditions. Tangential diffusers direct the fluid along a spiral path, enabling efficient pressure recovery while retaining kinetic energy, thereby making them suitable for high-pressure, high-efficiency applications [5]. In contrast, radial diffusers guide the flow outward from the impeller and generally convert more kinetic energy into pressure energy, resulting in more stable flow conditions at lower pressures [6]. An effective volute design must deliver uniform flow around the pre-distributor and minimize internal losses.

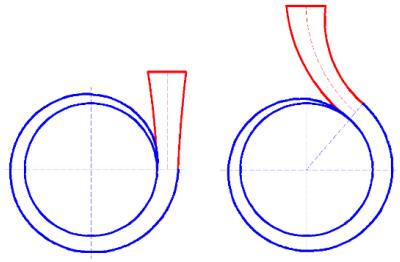

a) b)

Figure 1

Types of diffusers a) tangential b) radial diffusers

The primary distinction between tangential and radial diffuser designs lies in the direction in which they guide the fluid. As shown in Figure 1, a radial diffuser directs the fluid radially outward, promoting efficient conversion of kinetic energy to pressure, whereas a tangential diffuser directs it tangentially. The pump's performance characteristics are strongly influenced by its orientation. According to the literature, the radial diffuser design is typically applied in cases with higher flow rates and smaller pressure differentials [7-9]. It is oriented to direct the fluid radially toward the pump outlet. In this design, the radial diffuser converts fluid energy into rotational motion, creating a pressure differential. The radial diffuser is typically

preferred in pumps with low specific speed and high head, whereas the tangential diffuser is advantageous at higher specific speeds because it accommodates stronger tangential flow components.

Alemi et al. [9] examined the influence of volute shape on the head, effectiveness, and radial force of a low-specific-speed centrifugal pump. They evaluated the effects of different volute design methods and geometries on performance. They stated that both tangential and radial diffusers provide approximately the same head; however, at high flow rates, the radial diffuser is slightly more efficient. Furthermore, they deduced that at low flow rates, the radial diffuser generates a smaller radial force. Chalghoum et al. [7] studied the impact of the volute diffuser geometry on pressure fluctuations in centrifugal pumps. They aimed to analyze, using radial and tangential diffusers, the characteristics of pressure fluctuations under different flow rates for the same impeller. Radial diffuser pumps provided lower pressure-surge amplitudes than pumps using tangential diffusers. Their analysis showed that the shape of the volute diffuser affects the pressure fluctuations.

Other research has explored additional geometric and unsteady flow aspects. Zhang et al. [10] reviewed the detrimental effects of pressure fluctuations on pump vibration and stress, identifying rotor–stator interaction as a primary cause. Dehghan and Shojaeefard [11] investigated the importance and effect of volute design in centrifugal pumps. Different volute parameters, cross-sectional shapes, and design theories were analyzed experimentally and numerically. The results indicated that the volute with a circular cross-section was the most efficient, the theory of the conservation of angular momentum was the most suitable design approach, and the specific cutwater angle and diameter produced the highest efficiency. Belbachir et al. [6] investigated the mechanical properties of different types of volutes in a centrifugal pump. They showed that stress was concentrated at the volute nozzle, and that the tangential diffuser experienced less stress than other diffuser types. Meng et al. [12] conducted a numerical investigation of the impeller–volute interaction, which they identified as one of the main causes of high-pressure fluctuations in centrifugal pumps. Through numerical simulations, they analyzed the effects of radial and tangential diffusers on volute geometry. They stated that pressure fluctuations significantly affected pump performance, vibration, stability, and noise. They found that the pressure fluctuation amplitudes for the radial diffuser pump were lower than those for the tangential diffuser pump.

Additional advances include optimization of radial gap size [13]; empirical and analytical diffuser design methods; advanced turbulence modeling for rotating stall characterization [14]; diffuser wrap-angle optimization, which improves efficiency by up to 4% [15]; return-guide-vane outlet-angle modifications, which increase head by nearly 20% [[16]; and the 3D impeller-outflow instability model proposed by Fan et al. [17], which improves identification of unsteady structures at the diffuser inlet. [17] Reduced diffuser-vane heights have also been shown to suppress small-scale vortices and decrease volute hydraulic loss [18]. Studies on ultra-low-

specific-speed pumps [19], geometric influences on pulsations [20], unsteady-flow characterization [21], and double-volute pressure balancing [22] consistently demonstrate that diffuser and adjacent geometry significantly affect head, unsteady forces, and upstream inlet conditions. However, despite these advances, direct numerical comparisons of radial and tangential diffusers across a range of specific speeds under identical impeller and operating conditions remain limited.

Specific speed is a dimensionless parameter, calculated using Equation (1), that characterizes pump performance based on flow rate (Q), head (H), and rotational speed (n).

$$n_q = \frac{n\sqrt{Q}}{(H)^{3/4}} \tag{1}$$

where nq represents specific speed (dimensionless), n, Q, and H are the pump's rated speed, flow rate, and pressure head, respectively. It governs the impeller geometry and the relative distribution of kinetic and pressure energy at the impeller outlet. Increasing specific speed leads to a transition from radial to mixed-flow and eventually axial-flow impeller behavior [23]. The pressure coefficient (C_p), used in evaluating pressure fluctuations, is defined as:

$$C_p = \frac{p - p_{ref}}{0.5\rho V_{ref}^2} \tag{2}$$

where p is the local static pressure, $Pref$ is the reference pressure (typically the inlet pressure), ρ is the fluid density, and V_{ref} is the reference velocity (impeller tip speed). This parameter facilitates comparison across different operating conditions by normalizing pressure variations.

Centrifugal pumps are typically categorized into radial-, mixed-, and axial-flow types based on specific speed [23]. Lower specific speeds correspond to radial impellers, while higher specific speeds correspond to mixed and axial configurations. Although the literature includes several studies comparing radial and tangential diffusers, most focus on a single pump or a single operating condition, often emphasizing mechanical behavior, pressure fluctuations, or efficiency.

Despite extensive studies on volute geometry and unsteady flow, to the best of the authors' knowledge, no prior study has systematically compared radial and tangential diffusers across the specific-speed range of n_q : 19-42 using identical impeller geometry and operating conditions. The present study expands upon existing research by numerically analyzing three radial-flow centrifugal pumps with specific speeds of 19 (high-pressure), 27 (medium-pressure) and 42 (low-pressure). The models share identical impeller geometry and operate under the same design head (20 m) and rotational speed (2800 rpm), ensuring that any performance differences arise solely from diffuser type and specific speed. The analysis separately evaluates low-, medium-, and high-specific-speed pumps to isolate

diffuser-induced effects on head development, unsteady flow characteristics, and hydrodynamic forces. This work is novel because no prior study has systematically compared radial and tangential diffusers over the specific-speed range of 19-42, under identical geometric and operating constraints, thereby filling a significant gap in the literature and providing practical guidance for improving efficiency and stability across a wide range of pump applications.

2 Numerical Method

Numerical simulations were conducted using, Simcenter Star CCM+ 2406, to investigate flow dynamics in centrifugal pumps. The simulation employed a time-dependent Rigid Body Motion (RBM) framework to capture interactions between rotating and stationary components. In this setup, the pump casing walls were stationary, while the impeller's rear plate was modeled as a rotating boundary. The internal flow was considered incompressible, turbulent, and quasi-steady; the RNG (Renormalization Group) k-ε turbulence model was employed. This model is suitable for flows with high strain rates and significant streamline curvature, effectively accounting for rotation effects within the averaged flow field [24] [25].

The flow equations were solved using the SIMPLE (Semi-Implicit Method for Pressure-Linked Equations) algorithm, which iteratively couples the pressure and velocity fields to solve the Navier–Stokes equations [26]. A segregated solver was used to solve the momentum and continuity equations sequentially, with first-order spatial discretization and implicit time integration to ensure numerical stability and convergence [27]. Simulations can be reproduced by importing the pump geometries (Figure 5), applying the RNG k-ε turbulence model using water as the working fluid (density ρ : 997.5 kg/m³, viscosity μ : 8.87 × 10^{-4} Pa·s), and running unsteady simulations with the specified time step.

To improve near-wall prediction accuracy, a two-layer, all-y^+ wall treatment was implemented, maintaining $y^+ < 1$ to resolve both the viscous sublayer and the turbulent buffer layer. An appropriately small time step (Δt : 10^{-5} s) was chosen to capture unsteady phenomena such as blade-passing effects, sudden pressure fluctuations, and rapid fluid motion. For an impeller operating at 2800 rpm with six blades, this time step ensures more than 350 increments per blade passage, enabling high-fidelity resolution of transient flow interactions [27].

The governing equations used in the analysis included the time-averaged continuity equation and the Navier–Stokes equations in the relative coordinate system. The Navier-Stokes equations are fundamental relations that describe fluid motion. In systems with complex geometries, such as radial and tangential diffusers, these equations are used to calculate the velocity and pressure distributions of the fluid.

Continuity Equation

The continuity equation represents the conservation of mass. For incompressible flow, it is expressed as follows:

$$\nabla . u = 0 \tag{3}$$

where u is the fluid velocity vector.

Momentum Equation

The momentum equation , which describes changes in fluid velocity, is typically derived from Newton's second law. In the study of motion in a rotating reference frame, fictitious centrifugal and Coriolis forces are added to the right-hand side of the momentum equations to account for rotational motion. The momentum equation can be defined as follows:

$$\frac{\partial(\rho u)}{\partial t} + \nabla . (\rho u \otimes u) = -\nabla p + \nabla . \tau + \rho g - 2\rho \mathrm{w} \times u - \rho \mathrm{w} \times (\mathrm{w} \times r) \tag{4}$$

The Coriolis ($2\rho \mathrm{w} \times u$) and centrifugal forces ($\rho w \times (\mathrm{w} \times r)$) are incorporated into the momentum equations. These equations enable a more precise modeling of the flow in a rotating reference frame. The stress tensor (τ) is defined as:

$$\tau = \mu \left(\nabla u + (\nabla u)^T - \frac{2}{3} (\nabla . u) I \right) \tag{5}$$

where ρ, p, and μ represent fluid density, pressure, and dynamic viscosity, respectively, and g denotes gravity. The variables t, τ, w, and r refer to time, stress tensor, angular velocity, and position vector, respectively.

Hydrodynamic Force

The total hydrodynamic force acting on a solid surface is obtained by summing the pressure and shear contributions over all surface faces:

$$F = \sum_{D} \left(F_{pressure,D} + F_{shear,D} \right) \tag{6}$$

The pressure force acting on a surface face D is computed as:

$$F_{pressure,D} = \left(p_s - p_{ref} \right) \cdot A_D \tag{7}$$

where p_s and p_{ref} are the static and reference pressures, respectively. A_D is the area vector of the surface. The shear force on the surface is computed as:

$$F_{shear,D} = -\tau_D \cdot A_D \tag{8}$$

In this study, the hydrodynamic forces acting on the impeller and the volute were extracted during post-processing using Simcenter STAR-CCM+. The complete wetted surface of each component was selected, and the local pressure and shear stress fields were integrated according to Equations (6)-(8) to obtain the net forces.

2.1 Validation Studies

Experimental data obtained from [28] were employed to validate the simulations, as shown in Figure 2. The reference pump operated at a flow rate of 40 m³/h, a head of 30 m, and an impeller speed of 2850 rpm. A corresponding centrifugal pump model was created, with mesh and physical conditions set to match these experimental parameters. Simulations were then performed under identical conditions; the head values at flow rates of 30.38, 40.59, and 46.90 m³/h were used for validation.

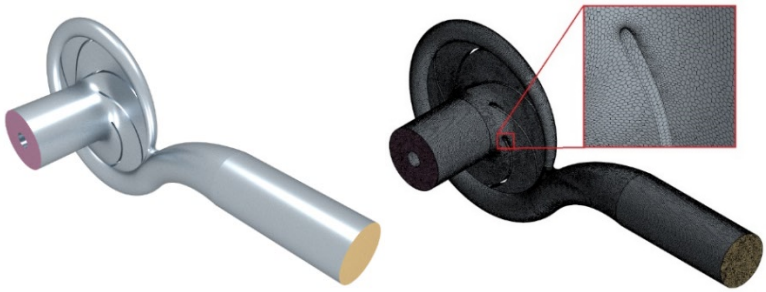

Figure 2
Geometry and mesh domains for the validation case, based on the experimental data from [28]

Figures 3 and 4 show the head and C_p distributions of the validated pump. The head obtained from the simulations slightly exceeded that obtained from the experiments. The deviation rates between the experimental and simulated results are valid across different flow rates, as shown in Figure 3. The deviation rate was lowest at low flow rates and increased slightly as flow rate increased. Unaccounted leakage and mechanical losses caused these deviations and affected the experimental results. In [28], a similar trend was observed: their simulations produced values higher than those of the experiments. In this validation study, the error rate ranged from 3.2% to 12.9%. An acceptable discrepancy of approximately 8.8% was observed at the highest efficiency (BEP) flow rate for the validated pump. The residual discrepancy (3.2-12.9%) is attributed mainly to experimental unmodelled leakage, mechanical losses, and slight geometric differences; similar trends were also reported in [28].

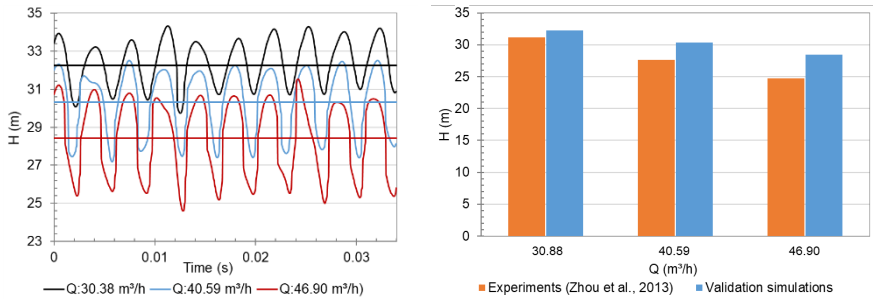

a) b)

Figure 3

a) Head of the validated centrifugal pump examined by [28] (b) Deviation rates at different flow rates

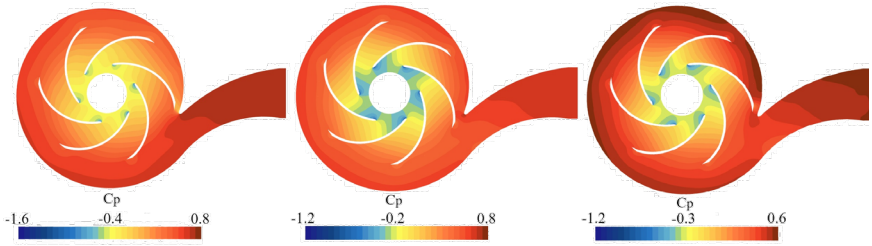

a) b) c)

Figure 4

Pressure coefficient (C_p) distributions at the mid-plane for the validated centrifugal pump examined by [28]; a) Q:30.38 m^3/h; b) Q:40.59 m^3/h; c) Q:46.90 m^3/h

2.2 Computational Domains

The computational domains of radial and tangential centrifugal pumps with a specific speed of n_q : 19 are illustrated in Figure 5 Each pump consists of four main components: inlet channel, impeller, volute, and outlet channel. To improve flow uniformity, the inlet (suction duct) was extended by 100 mm, while the outlet (pressure duct) was extended by 175 mm. These extensions promote gradual and stable flow entry and exit, reducing turbulence and energy losses, and enhancing overall pump performance[29].

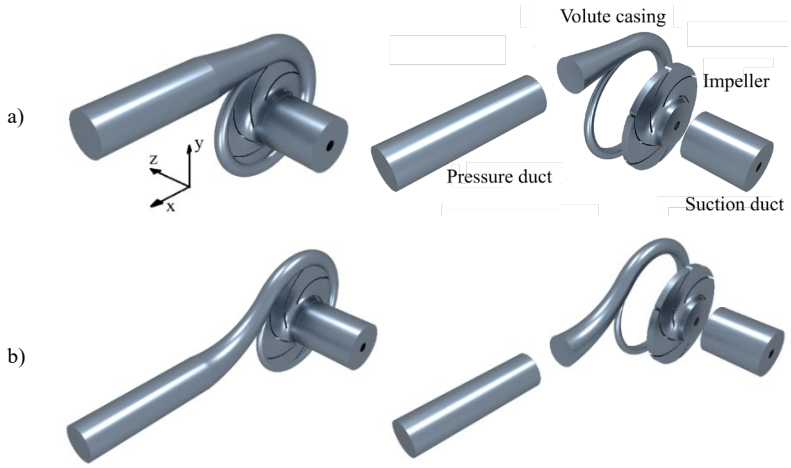

Figure 5
Computational domains of a) radial and b) tangential diffusers in a centrifugal pump with a specific speed of n_q:19

Three pump designs with specific speeds of 19 (250 L/min), 27 (500 L/min), and 42 (1200 L/min) were analyzed (Table 1). A constant head of 20 m and a rotational speed of 2800 rpm were maintained for all designs. Although all pumps were radial-flow types, they were classified as high-pressure (n_q: 19), medium-pressure (n_q: 27), and low-pressure (n_q: 42) variants. Each impeller had six blades; additional properties are summarized in Table 1.

Table 1
Impeller properties

Impeller dimensions	**250 l/min**	**500 l/min**	**1200 l/min**
General type	**Low flowrate High pressure**	**Medium flowrate Medium pressure**	**High flowrate Low pressure**
Specific speed	19	27	42
Blade number	6	6	6
Hub diameter (mm)	11.69	14.15	18.43
Suction diameter (mm)	57.2	69	88.1
Outlet diameter (mm)	132.2	136.3	144.3
Outlet width (mm)	8.46	11.18	16.31

2.3 Boundary Conditions and Mesh Domain

Three centrifugal pumps with different specific speeds were examined numerically. To ensure a radial-flow configuration, specific speeds (n_q) for the radial-flow pump were categorized as follows: low (n_q: 19), medium (n_q: 27), and high (n_q: 42).

A stagnation inlet boundary condition was applied at the pump inlet, as shown in Figure 6a. The stagnation inlet refers to the conditions at a hypothetical point in the flow where the fluid comes to a complete stop before entering the system. Stagnation conditions encompass parameters such as stagnation pressure, stagnation temperature, and flow direction. These parameters account for both the static and velocity pressure effects of the flowing fluid. A mass flow outlet condition was employed at the outlet boundary, allowing the fluid to exit the computational domain at the specified flow rate, as shown in Figure 6a. The pump's walls were modelled with no-slip boundary conditions, indicating that there was no relative motion between the fluid and solid surfaces. In addition, to enable smooth communication and flow transfer between components, an interface boundary condition was defined at both the impeller–inlet channel intersection and the impeller–volute interface, as depicted in Figure 6b.

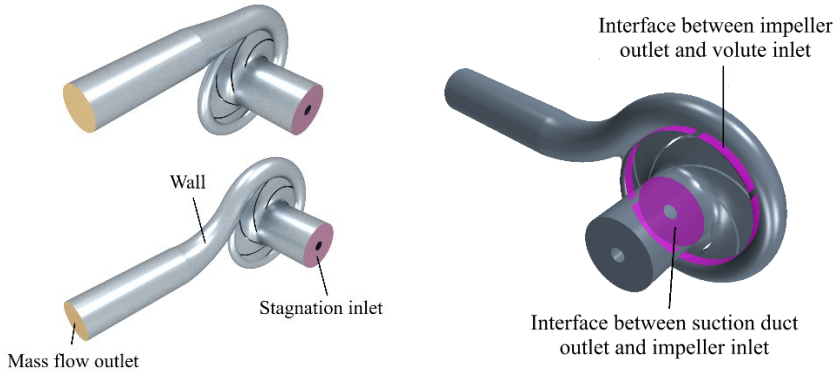

Figure 6
Boundary conditions and interfaces of the pump at a specific speed n_q:27

A high-quality polyhedral mesh was generated for all computational domains, including the impeller, volute, and inlet regions, as depicted in Figure 7. The mesh quality diagnostics confirmed that the mesh was fully valid, with no negative-volume cells and 100% face validity across all regions. The maximum skewness angle remained below 80°, which is acceptable for rotating machinery simulations in Star-CCM+. The minimum distance between neighboring cell centroids was on the order of 2.4×10^{-5} m, ensuring adequate spatial resolution near the blade leading and trailing edges.

A mesh independence study was performed using five refinement levels. Convergence was achieved at an average cell size of approximately 0.5 mm, when the pump head variation between successive refinements fell below 1%. All simulations therefore used this mesh density, which provides a balance between numerical accuracy and computational efficiency. Boundary-layer refinement with prism layers ensured that y^+ values remained within the valid range for the RNG k–ε turbulence model, enabling accurate prediction of near-wall flow behavior.

Figure 7
Mesh domain for specific speed n_q:19

3 Results and Discussions

Figure 8 shows the head fluctuations of the pump in the three cases. At low specific speeds (Figure 8a), fluctuations are significantly increased; they decrease as specific speed increases. In particular, at low specific speeds, a centrifugal pump with a radial diffuser provides a higher head, whereas at higher specific speeds a centrifugal pump with a tangential diffuser provides a higher head [30]. At a specific speed of 19, fluctuations are similar for both diffuser types. However, at specific speeds of 27 and 42 (Figures 8b and 8c), the radial diffuser exhibited slightly greater fluctuations. At a specific speed of 19, impeller-induced head fluctuations are more pronounced, but these fluctuations diminish as the specific speed increases. These fluctuations reach approximately 4 m, 2 m, and 0.5 m, respectively, for specific speeds of 19, 27 and 42, at their maximum and minimum values. This trend aligns with Chalghoum et al. [7], who reported lower pressure surge amplitudes in radial diffusers; however, our multi-speed comparison extends their single-impeller findings. Although the radial diffuser exhibits slightly higher instantaneous head fluctuations at n_q = 27 and 42, this behavior does not translate into higher hydrodynamic forces. Head fluctuation is a local pressure effect, whereas force response depends on the surface-integrated pressure distribution.

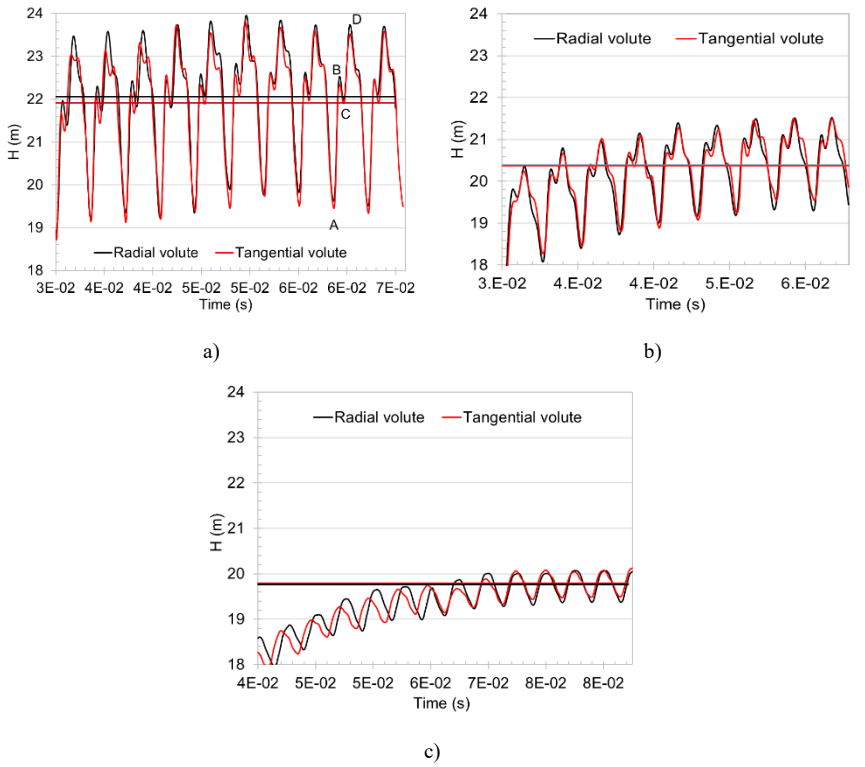

Figure 8

Head for radial and tangential diffusers at specific speeds; a) n_q:19; b) n_q:27; c) n_q:42

Figure 9 illustrates the impeller positions within the pump and the pressure distribution in the volute and the impeller during pressure fluctuations. The minimum pressure (Point A) occurs when the blade aligns with the cutwater in the tangential diffuser, whereas the corresponding position in the radial diffuser is Point B. The Maximum pressure occurs when the blade is farthest from the cutwater, at Point D for both diffusers. In contrast, in the radial diffuser, the cutwater region is located between the two blades. As the head increases, a small, abrupt decrease occurs at points B and C. This occurs when the blade moves away from the cutwater region in the tangential diffuser, whereas in the radial diffuser, it occurs when the blade passes through the cutwater region. For the highest head (Point D), in both volutes, the blade is situated away from the cutwater region. The maximum pressure in both diffusers occurs when the blade is at the cutwater, which is at Point A for the tangential diffuser and Point B for the radial diffuser. In conclusion, pressure fluctuations are more significant at low specific speeds [31]. In addition, both diffusers exhibit a similar pattern of pressure fluctuations, but these fluctuations occur at different blade positions across the range between the minimum and maximum pressure values.

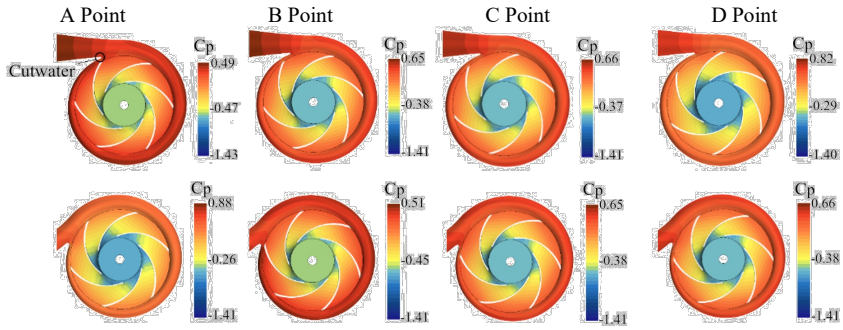

Figure 9
Pressure fluctuation conditions for n_q:19

Figure 10 displays the hydrodynamic forces acting on the volute for pumps equipped with radial and tangential diffusers. The coordinate system is defined such that the x-axis aligns with the volute-tongue direction, the y-axis lies in the radial direction within the meridional plane, and the z-axis corresponds to the shaft axis. Hydrodynamic forces were computed from Equations (6-8) by integrating pressure and shear stresses over the wetted volute surface during post-processing in STAR-CCM+. Components in the x- and y-directions constitute the radial force acting on the volute, whereas the z-component represents the axial force transmitted to the volute structure.

As shown in Figure 10, the radial components – particularly the x-component aligned with the volute tongue – dominate the volute loading, while axial components are relatively small. Increasing the specific speed amplifies the overall force magnitudes. At low specific speed (n_q = 19), pumps with radial and tangential volutes exhibit similar force levels and fluctuation patterns. However, at higher specific speeds, although fluctuation amplitudes remain comparable, the radial-volute configuration produces lower net force magnitudes on the volute than the tangential configuration. For n_q values of 19, 27 and 42, the pressure-induced force fluctuations acting on the volute are approximately 40 N, 10 N, and 20 N, respectively.

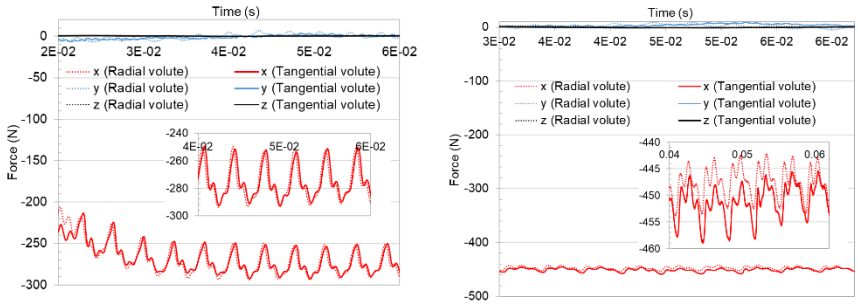

a) b)

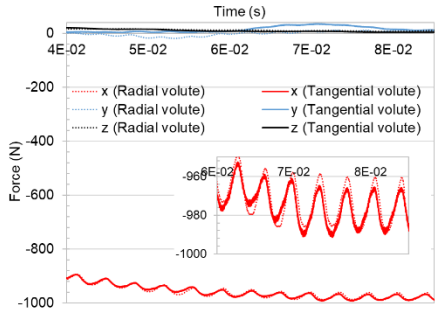

c)

Figure 10

Forces acting on the volute of the tangential and radial diffuser pumps at specific speeds; a) n_q:19; b) n_q:27; c) n_q:42

Figures 11a-c show the forces acting on the impeller at speeds of 19, 27 and 42, respectively. No significant radial force is generated by the impeller. The most prominent force acts in the z-direction, which is the axis along which the flow enters the pump. This force increases as speed increases. As depicted in Figure 11, the force in the z-direction is slightly higher for the radial diffuser than for the tangential diffuser in the high-specific-speed case (42). This force experiences minimal fluctuations. Although radial forces are low, larger fluctuations occur during impeller rotation. For the pump with a tangential diffuser, across all specific speeds, fluctuations are greater in the x-direction (the direction of fluid exit from the pump, i.e., the volute), whereas fluctuations in the y-direction are greater in the radial direction. While radial forces remain relatively low on average, larger unsteady fluctuations occur as the impeller rotates, driven by blade-passing and impeller–volute interactions [32].

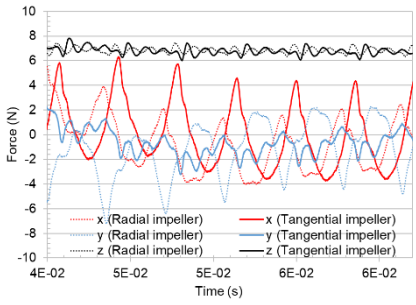

a)

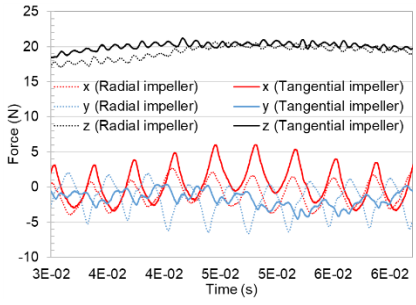

b)

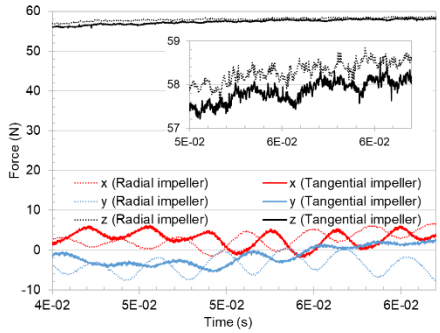

c)

Figure 11

Forces acting on the impeller of the tangential and radial diffuser pumps at specific speeds; a) n_q:19; b) n_q:27; c) n_q:42

Figures 12a and 12b show velocity vectors in the pump cross-sections for specific speeds of 19 and 42. For a pump with a lower specific speed, the flow directed toward the pump outlet is more uniform, especially with a radial diffuser. In this scenario, flow separation is slightly reduced, and velocities exhibit greater regularity. However, for a tangential diffuser, distinct flow separation occurs in the flow toward the outlet. The secondary flows and vortices generated in this region result in pressure losses, which are evident in the lower head depicted in Figure 8. In the high-specific-speed radial-flow centrifugal pump (Figure 12b), the flow vectors directed toward the pump outlet were smooth in both the radial-diffuser and tangential-diffuser cases. Consequently, the pressure losses are similar in both cases. This is evident from the roughly equal head heights shown in Figure 8.

a)

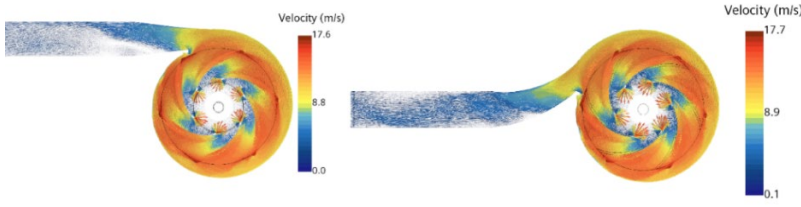

b)

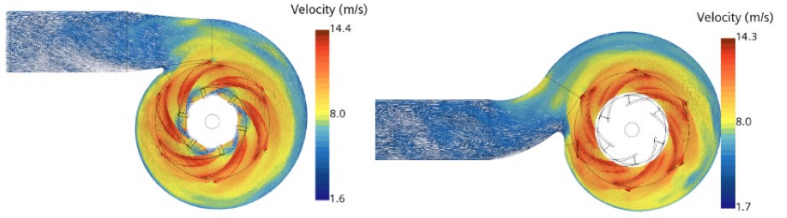

Figure 12

Velocity vector of the midplane of the pumps at specific speeds; a) n_q:19; b) n_q:42

Figure 13 presents velocity vectors in planes parallel and perpendicular to the volute outlet for both tangential and radial diffuser pumps. The velocity vectors near the impeller align in both tangential and radial diffuser cases and exhibit similar patterns. These similarities persist in both cases after passing through the water-cut section of the volute. However, as the flow approaches the volute outlet, a contrast becomes evident. For the tangential diffuser, the flow velocity is lower in the outer regions of the volute and higher in the central sections. In contrast, the radial diffuser exhibits a smoother velocity gradient at the volute outlet than that of the tangential diffuser. Although the flow in the volute occurs at lower velocities in its outer regions, these velocities are primarily confined to the outermost part. In the tangential diffuser, lower velocities create circular regions characterized by low-velocity vectors adjacent to the volute walls.

Figure 13
Velocity vector at the cross-section planes

Figure 14 depicts the radial velocity contours across the volute cross-section for both tangential and radial diffuser configurations. As the liquid flows toward the outlet in both cases, the radial velocities are approximately the same. In the radial diffuser, these radial velocities tend to concentrate in the region at the volute outlet where radial turning occurs. However, in the outer areas of the volute, where tangential velocities dominate the flow, radial velocities are not generated. This phenomenon results from the centrifugal force exerted on the liquid by the impeller blades, which leads to radial liquid movement. Radial velocities are visible at the blade tips, as shown in Figure 14. In the region between the two blades, the liquid is directed tangentially toward the outlet due to the prevailing tangential flow that extends throughout the volute.

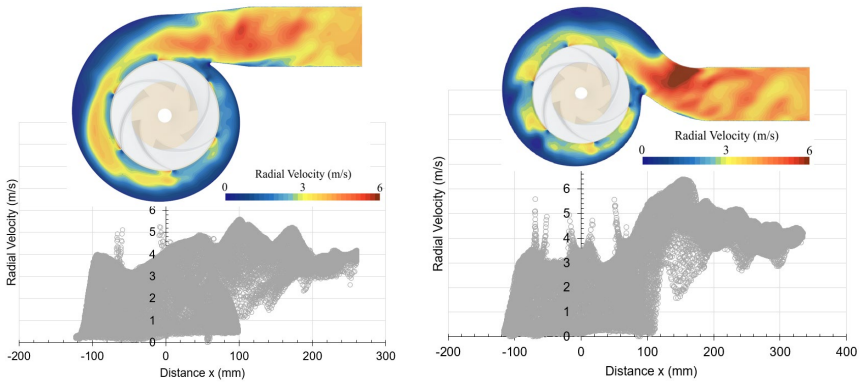

Figure 14

Radial velocity of a) tangential, b) radial diffuser pumps at specific speed n_q:42

Figure 15 presents the tangential velocities in both the tangential and radial diffuser configurations. Within the radial diffuser, tangential velocity develops minimally or not at all as the fluid flows toward the pump outlet. The rotation of the impeller at the blade tips imparts maximum tangential motion to the liquid. However, this tangential velocity decreases as it moves from the impeller toward the volute. Within the volute, the highest tangential velocity, found in the watercut region, gradually decreases as the volute expands toward a circular profile at the outlet. In the outer sections of the volute, the liquid is directed toward the outlet at lower tangential velocities. Consequently, when examining Figures 14 and 15 together, it becomes evident that at the volute outlet, the liquid exhibits a radial velocity rather than a tangential velocity. This radial velocity is higher in the radial-velocity pump.

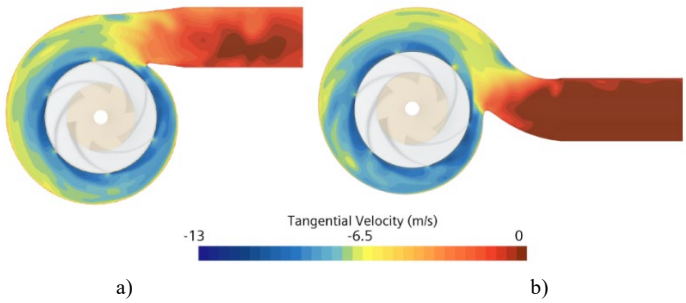

Figure 15

Tangential velocities of; a) tangential; b) radial diffuser pumps at specific speed n_q:42

Conclusions

In this numerical study, a comprehensive analysis of three radial-flow centrifugal pumps with different specific speeds – high-pressure (n_q: 19), medium-pressure (n_q:

27), and low-pressure (n_q: 42) – is conducted. All pumps exhibit radial-flow characteristics. The conclusions can be summarized as follows:

- At low specific speeds, head fluctuations reached approximately 4 m, while at higher specific speeds, these fluctuations decreased to approximately 0.5 m. This trend quantifies the stabilizing effect of increasing specific speed and is consistent with previous observations in the literature. For n_q : 19, the radial diffuser generated a higher head due to reduced flow separation, whereas at elevated specific speeds the tangential diffuser provides a slightly higher head by better accommodating stronger tangential flow components.
- Hydrodynamic force analysis revealed that, at low specific speeds, both diffusers produced nearly identical force levels and force fluctuations. Although instantaneous head fluctuations in the radial diffuser were slightly larger at higher specific speeds, the net hydrodynamic forces acting on the volute were lower for the radial diffuser than for the tangential diffuser. This distinction underscores that head variation and surface-integrated force response are governed by different physical mechanisms. Lower force levels in the radial diffuser may contribute to reduced volute loading and improved operational durability in relevant applications.
- In particular, at higher specific speeds, the forces generated in the volute increase notably, with fluctuations of up to 20 N. At low specific speeds (n_q:19), both radial and tangential diffusers exhibit approximately equal forces and fluctuations. However, at higher specific speeds, despite similar fluctuations across all volutes, the radial diffuser exerts lower forces than the tangential diffuser, thereby reducing wear in applications such as power generation.
- In the impeller, axial force remained the dominant component and increased with specific speed, while radial forces were comparatively small but exhibited periodic oscillations associated with blade-passing events. These unsteady behaviours highlight the importance of evaluating structural loads alongside hydraulic performance.
- In summary, diffuser selection should be based on specific-speed-dependent flow characteristics: radial diffusers are advantageous at low specific speeds because of reduced flow separation and lower force response, whereas tangential diffusers are more suitable at higher specific speeds, where tangential momentum is more pronounced. These findings provide practical design guidance for improving flow stability, hydraulic efficiency, and component reliability in industrial centrifugal pump applications.

Nomenclature

A	Area (m²)
A_D	Area vector of surface face D (m²)
BEP	Best Efficiency Point
CFD	Computational Fluid Dynamics

C_p	Pressure coefficient (dimensionless)
F	Resultant hydrodynamic force vector (N)
$F_{pressure,D}$	Pressure force on surface face D (N)
$F_{shear,D}$	Shear force on surface face D (N)
g	Gravitational acceleration vector (m/s²)
H	Head (m)
n	Rotational speed (rpm)
n_q	Specific speed (dimensionless)
p	Static pressure (Pa)
p_s	Surface static pressure (Pa)
p_{ref}	Reference pressure (Pa)
Q	Volumetric flow rate (m³/s or L/min)
RBM	Rigid Body Motion
RNG k–ε	Renormalization Group k–ε turbulence model
r	Position vector (m)
SIMPLE	Semi-Implicit Method for Pressure-Linked Equations
t	Time (s)
u	Velocity vector (m/s)
V_{ref}	Reference velocity (m/s)
w	Angular velocity vector (rad/s)
y^+	Dimensionless wall distance
Δt	Time step size (s)
μ	Dynamic viscosity (Pa·s)
ρ	Density (kg/m³)
τ	Viscous stress tensor (Pa)

References

[1] Karassik I J, Messina J P, Cooper P, Heald C C, York N, San C, Lisbon F, Madrid L, City M, New M, San D and Seoul J 2008 *Pump Handbook* (McGraw-Hill Education)

[2] Zhang Y, Hu S, Zhang Y and Chen L 2014 Optimization and Analysis of Centrifugal Pump considering Fluid-Structure Interaction *Scientific World Journal* **2014** 1-9

[3] Sulzer Pumps 2010 Principal Features of Centrifugal Pumps for Selected Applications *Centrifugal Pump Handbook* 251-83

[4] Wang T, Yu H, Fang Y, Xiang R, Kan N and Yan J 2022 A new design for energy-saving volutes in centrifugal pumps *Physics of Fluids* **34**

[5] Chen W, Li Y, Liu Z and Hong Y 2023 Understanding of energy conversion and losses in a centrifugal pump impeller *Energy* **263** 125787

[6] Belbachir S, Allali A, Lousdad A, Boucham B and Alami A 2023 Comparative analysis of the mechanical behavior of three volute forms of centrifugal pump *Journal of Fundamental and Applied Sciences* **14** 383-90

[7] Chalghoum I and Sami E 2020 Analysis the effect of the volute diffuser on unsteady pressure pulsation in a centrifugal pump at large operating conditions *International Journal of Theoretical and Applied Mechanics* **5** 82-9

[8] Chalghoum I, Bettaieb N and Elaoud S 2018 Effect of the volute diffuser shape on pressure pulsations and radial force in centrifugal pumps *Lecture Notes in Mechanical Engineering* **0** 603-12

[9] Alemi H, Nourbakhsh S A, Raisee M and Najafi A F 2015 Effects of volute curvature on performance of a low specific-speed centrifugal pump at design and off-design conditions *J Turbomach* **137** 041009

[10] Zhang N, Li D, Gao B, Ni D and Li Z 2023 Unsteady Pressure Pulsations in Pumps—A Review *Energies (Basel)* **16** 150

[11] Dehghan A A and Shojaeefard M H 2022 Experimental and numerical optimization of a centrifugal pump volute and its effect on head and hydraulic efficiency at the best efficiency point *Proc Inst Mech Eng C J Mech Eng Sci* **236** 4577-98

[12] Meng F, Pei J, Yuan S, Luo Y and Chen J 2016 Effect of two diffuser types of volute on pressure fluctuation in centrifugal pump under part-load condition *16th International Symposium on Transport Phenomena and Dynamics of Rotating Machinery* (Honolulu) p hal-01891318f

[13] Ooi K T, Dumitrescu O, Strătilă S and Drăgan V 2025 Design Methods and Practices for Centrifugal Compressor Diffusers: A Review *Machines 2025, Vol. 13, p. 990* **13** 990

[14] Alubokin A A, Gao B, Ning Z, Yan L, Jiang J and Quaye E K 2022 Numerical simulation of complex flow structures and pressure fluctuation at rotating stall conditions within a centrifugal pump *Energy Sci Eng* **10** 2146-69

[15] Liu Y Y, Yang G, Xu Y, Peng F and Wang L Q 2020 Effect of space diffuser on flow characteristics of a centrifugal pump by computational fluid dynamic analysis *PLoS One* **15** e0228051

[16] Górecki J, Klimentov K, Popov G, Kostov B and Ibrahim S 2024 Studying the Impact of Diffuser Return Guide Vanes on the Energy Performance of a Multistage Centrifugal Pump *Applied Sciences 2024, Vol. 14, p. 10991* **14** 10991

[17] Fan M, Dazin A, Bois G and Romanò F 2023 Instabilities identification based on a new centrifugal 3D impeller outflow model *Aerosp Sci Technol* **140** 108466

[18] Liu Z, Zhu X, Liu J, Kim M K and Jiang W 2024 A Numerical Investigation of the Influence of Diffuser Vane Height on Hydraulic Loss in the Volute

for a Centrifugal Water Supply Pump *Buildings 2024, Vol. 14, p. 2296* **14** 2296

[19] Wei Y, Shi Y, Shi W and Pan B 2022 Numerical Analysis and Experimental Study of Unsteady Flow Characteristics in an Ultra-Low Specific Speed Centrifugal Pump *Sustainability 2022, Vol. 14, p. 16909* **14** 16909

[20] Spence R and Amaral-Teixeira J 2009 A CFD parametric study of geometrical variations on the pressure pulsations and performance characteristics of a centrifugal pump *Comput Fluids* **38** 1243-57

[21] González J and Santolaria C 2006 Unsteady Flow Structure and Global Variables in a Centrifugal Pump *J Fluids Eng* **128** 937-46

[22] Kibar A and Yigit K S 2024 Investigation of double-volute balancing in centrifugal pumps *Meccanica* **59** 1859-75

[23] Karassik I J and McGuire T 1998 *Centrifugal Pumps* (Berlin/Heidelberg: Springer Science & Business Media)

[24] Zhou W, Yu D, Wang Y, Shi J and Gan B 2023 Research on the Fluid-Induced Excitation Characteristics of the Centrifugal Pump Considering the Compound Whirl Effect *Facta Universitatis, Series: Mechanical Engineering* **21** 223-38

[25] Mahdi M, Rasekh M and Sajadi V 2022 Unsteady Fluid Flow Analysis of Tongue Geometry in a Centrifugal Pump at Design and Off-design Conditions *Journal of Applied Fluid Mechanics* **15** 1851-67

[26] Patankar S V. and Spalding D B 1972 A calculation procedure for heat, mass and momentum transfer in three-dimensional parabolic flows *Int J Heat Mass Transf* **15** 1787-806

[27] Korkmaz Y S, Kibar A and Yigit K S 2021 Experimental and Numerical Investigation of Flow in Hydraulic Elbows *Journal of Applied Fluid Mechanics* **14** 1136-46

[28] Zhou L, Shi W and Wu S 2013 Performance optimization in a centrifugal pump impeller by orthogonal experiment and numerical simulation *Advances in Mechanical Engineering* **2013** 385809

[29] Yun L, Yuan X, Zhen Z, Rui W, Rongsheng Z and Qiang F 2024 Study on cavitation flow and high-speed vortex interference mechanism of high-speed inducer centrifugal pump based on full flow channel *Journal of the Brazilian Society of Mechanical Sciences and Engineering 2024 46:12* **46** 1-19

[30] Zhao W, Wang M, Liang B, Zhao L and Liu Q 2024 Study of transient pressure and fluctuation characteristics in a centrifugal pump using the delayed detached-eddy simulation method *Intelligent Marine Technology and Systems 2024 2:1* **2** 1-20

[31] Wei Y, Zhu H, Fan Q, Qiu N, Wu J and Zhang W 2024 Numerical Study of Low-Specific-Speed Centrifugal Pump Based on Principal Component Analysis *Water 2024, Vol. 16, p. 1785* **16** 1785

[32] Zhang H, Li K, Liu T, Liu Y, Hu J, Zuo Q and Jiang L 2025 Analysis the Composition of Hydraulic Radial Force on Centrifugal Pump Impeller: A Data-Centric Approach Based on CFD Datasets *Applied Sciences 2025, Vol. 15, p. 7597* **15** 7597